

# Influence of turbulence model constants and boundary conditions on the computed hydrodynamic variables in gas-stirred reactors

T. Deb Roy

*Department of Materials Science and Engineering, The Pennsylvania State University, University Park, Pennsylvania, USA*

A. K. Majumdar

*CHAM of North America, Inc., Huntsville, Alabama, USA  
(Received June 1982; revised November 1982)*

A finite difference procedure has been employed to obtain numerical predictions of recirculating flows in gas-stirred reactors. Sensitivity of alternative boundary conditions at gas-liquid interface as well as empirical constants of the turbulence model on the predicted flow field have been investigated.

**Key words:** mathematical model, turbulence, gas-stirred reactors

## Introduction

In recent years there has been a growing interest in the numerical prediction of fluid flow in gas-stirred reactors.<sup>1-4</sup> In many of these studies the gas-liquid interaction was represented by (1) identifying arbitrarily a surface sufficiently distant from the axis as the interface between the two phase gas-liquid region and the single phase liquid region, and (2) prescribing a measured velocity distribution at that surface as a boundary condition. Both these prescriptions are somewhat difficult to meet in practice.

Deb Roy, Majumdar and Spalding<sup>1</sup> have earlier proposed a method to predict the fluid flow in the single phase liquid region without prescribing the measured velocity distribution at the liquid/two phase mixture interface. It was demonstrated that the flow field could be predicted with reasonable accuracy by using only the gas flow rate data. Recently Deb Roy and Majumdar<sup>2</sup> examined the effect of variation of the size of the two phase region (or the location of the said interface plane) on the predicted velocity profile in the liquid region. It was found that in most parts of the flow domain away from the axis, the predicted velocity field was not significantly influenced by the variation of the size of the two phase region.

The general approach adopted by the earlier workers has been the prediction of single phase fluid flow through

solutions of equations of continuity, momentum and other equations governing the turbulence properties such as the kinetic energy of turbulence and its dissipation rate. There are two basic problems associated with such treatments. First, it is necessary to prescribe boundary conditions of the turbulence quantities at the two phase/liquid interfaces, a task which is not straightforward. Secondly, even the most sophisticated turbulence model available today contains a number of so-called 'constants' which are not fundamental constants but are experimentally determined values obtained from idealized and simple experiments. The validity of these constants in recirculating flows have not been fully established.

Since the quality of the predicted velocity profiles is affected by the prescriptions of the boundary conditions of the turbulence quantities and also by the magnitude of the empirical constants contained in the models, this paper contains a solution of computed results to examine these two aspects.

## Governing equations

Flows are assumed to be axisymmetric and single phase. Turbulence is represented by an effective viscosity ex-

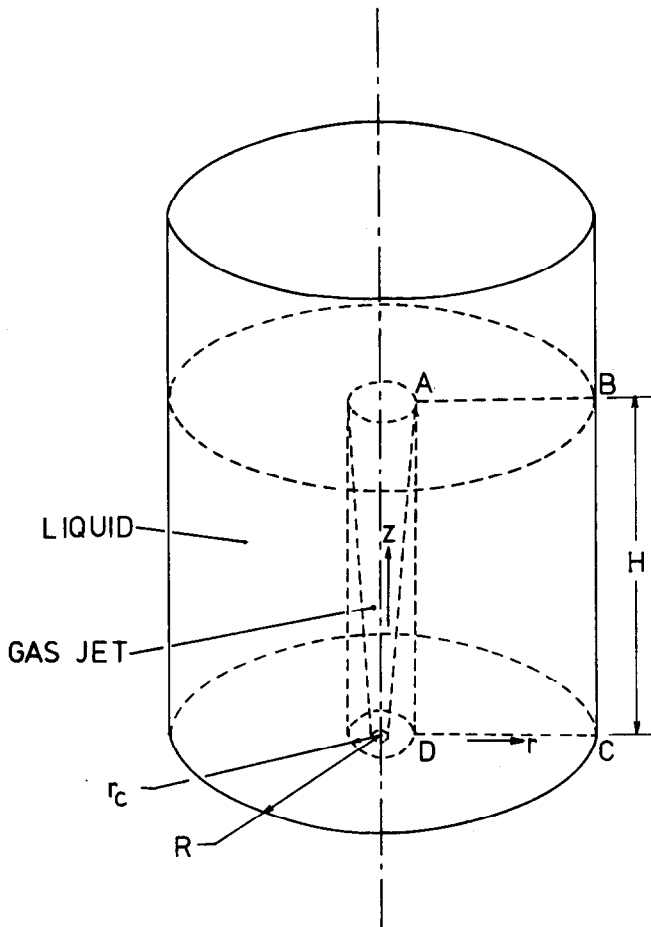


Figure 1 Schematic diagram of experimental situation

pressed as a function of turbulence energy and dissipation rate.

With reference to the coordinate system shown in Figure 1, the equations to be solved are:

Continuity:

$$\frac{\partial}{\partial z}(\rho u) + \frac{1}{r} \frac{\partial}{\partial r}(\rho r v) = 0 \quad (1)$$

Momentum:

z direction:

$$\begin{aligned} \frac{\partial}{\partial z}(\rho u^2) + \frac{1}{r} \frac{\partial}{\partial r}(\rho r v u) \\ = -\frac{\partial p}{\partial z} + \frac{\partial}{\partial z} \left( \mu_{\text{eff}} \frac{\partial u}{\partial z} \right) + \frac{1}{r} \frac{\partial}{\partial r} \left( r \mu_{\text{eff}} \frac{\partial u}{\partial r} \right) + S_u \end{aligned} \quad (2)$$

where:

$$S_u = \frac{\partial}{\partial z} \left( \mu_{\text{eff}} \frac{\partial u}{\partial z} \right) + \frac{1}{r} \frac{\partial}{\partial r} \left( \mu_{\text{eff}} r \frac{\partial v}{\partial r} \right)$$

r direction:

$$\begin{aligned} \frac{\partial}{\partial z}(\rho u v) + \frac{1}{r} \frac{\partial}{\partial r}(\rho r v^2) \\ = -\frac{\partial p}{\partial r} + \frac{\partial}{\partial z} \left( \mu_{\text{eff}} \frac{\partial v}{\partial z} \right) + \frac{1}{r} \frac{\partial}{\partial r} \left( r \mu_{\text{eff}} \frac{\partial v}{\partial r} \right) + S_v \end{aligned} \quad (3)$$

where:

$$S_v = \frac{\partial}{\partial z} \left( \mu_{\text{eff}} \frac{\partial v}{\partial z} \right) + \frac{1}{r} \frac{\partial}{\partial r} \left( r \mu_{\text{eff}} \frac{\partial v}{\partial r} \right) - \frac{2v\mu_{\text{eff}}}{r^2}$$

Turbulence energy:

$$\begin{aligned} \frac{\partial}{\partial z}(\rho u k) + \frac{1}{r} \frac{\partial}{\partial r}(\rho r v k) \\ = \frac{\partial}{\partial z} \left( \frac{\mu_{\text{eff}}}{\sigma_k} \frac{\partial k}{\partial z} \right) + \frac{1}{r} \frac{\partial}{\partial r} \left( r \frac{\mu_{\text{eff}}}{\sigma_k} \frac{\partial k}{\partial r} \right) + S_k \end{aligned} \quad (4)$$

where:

$$S_k = G - \rho \epsilon \quad (5)$$

$$G = \mu_t \left[ 2 \left\{ \left( \frac{\partial u}{\partial z} \right)^2 + \left( \frac{\partial v}{\partial r} \right)^2 + \left( \frac{v}{r} \right)^2 \right\} + \left( \frac{\partial u}{\partial r} + \frac{\partial v}{\partial z} \right)^2 \right] \quad (6)$$

Dissipation rate of turbulence energy:

$$\begin{aligned} \frac{\partial}{\partial z}(\rho u \epsilon) + \frac{1}{r} \frac{\partial}{\partial r}(\rho r v \epsilon) \\ = \frac{\partial}{\partial z} \left( \frac{\mu_{\text{eff}}}{\sigma_\epsilon} \frac{\partial \epsilon}{\partial z} \right) + \frac{1}{r} \frac{\partial}{\partial r} \left( r \frac{\mu_{\text{eff}}}{\sigma_\epsilon} \frac{\partial \epsilon}{\partial r} \right) + S_\epsilon \end{aligned} \quad (7)$$

$$S_\epsilon = \frac{C_1 \epsilon G}{k} - \frac{C_2 \rho \epsilon^2}{k} \quad (8)$$

The expression for  $\mu_{\text{eff}}$  is:

$$\mu_{\text{eff}} = \mu_l + C_D \rho k^2 / \epsilon \quad (9)$$

The model contains five empirical constants which are assigned the following typical values<sup>5</sup>:

$C_1$	$C_2$	$\sigma_k$	$\sigma_\epsilon$	$C_D$
1.43	1.92	1.0	1.3	0.09

#### Boundary conditions

For the flow situation shown in Figure 1, the boundary conditions are as follows:

At  $r = r_c$  (line AD in Figure 1)

$$u = U(z) \quad (10)$$

$$v = 0 \quad (11)$$

where  $U(z)$  is the measured<sup>3</sup> velocity distribution at  $r = r_c$ .

The prescription of turbulence quantities ( $k$  and  $\epsilon$ ) at  $r = r_c$  is not obvious. Therefore, three different sets of boundary conditions were employed to study their effect on the overall flow pattern as well as on the turbulence quantities themselves. They are as follows:

#### Test case A

The gradients of  $k$  and  $\epsilon$  at  $r = r_c$  are set to zero, i.e.:

$$\frac{\partial k}{\partial r} = 0 \quad (12)$$

$$\frac{\partial \epsilon}{\partial r} = 0 \quad (13)$$

Two additional test cases have been selected where turbulence quantities are specified arbitrarily at  $r = r_c$ .

Test case B

Turbulence energy ( $k$ ) has been prescribed to be 20% of the local value of kinetic energy, i.e.:

$$k = \alpha \frac{1}{2} U(z)^2 \tag{14}$$

where  $\alpha = 0.2$ . The dissipation rate of turbulence ( $\epsilon$ ) has been determined from the following expression<sup>6</sup>:

$$\epsilon = \frac{C_D k^{3/2}}{(0.03R)} \tag{15}$$

Test case C

Turbulence energy ( $k$ ) has been presumed to be 10% of the local value of kinetic energy, i.e.  $\alpha$  in equation (14) has been taken as 0.1. The value of  $\epsilon$  has been calculated from equation (15).

Free surface (line AB in Figure 1)

$$u = 0 \quad \frac{\partial v}{\partial z} = 0 \quad \frac{\partial k}{\partial z} = 0 \quad \frac{\partial \epsilon}{\partial z} = 0 \tag{16}$$

Walls (line DC and BC in Figure 1)

$$u = v = 0$$

Since close to the solid walls, the variation of flow properties are much steeper, the momentum ( $u, v$ ) and scalar ( $k, \epsilon$ ) transport processes have been modelled through wall functions.<sup>6</sup> A detailed discussion of this concept has been provided by Launder and Spalding,<sup>5</sup> and its application in two-dimensional recirculating flows appear in reference 6.

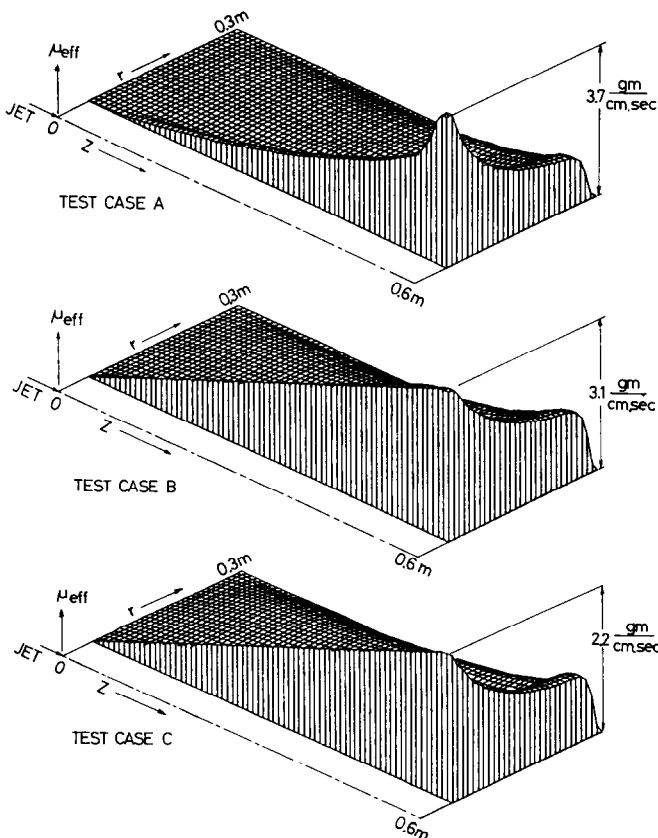


Figure 2 Predicted effective viscosity distribution for tests cases A, B and C

Table 1 Predicted values of  $u/u$  at  $r=r_c$  for different boundary conditions of  $k$  and  $\epsilon$

Test case	z/H	r/R			
		0.24	0.46	0.71	0.93
A	0.29	0.40	0.46	0.71	-0.20
	0.48	0.44	0.12	0.01	-0.19
	0.75	0.52	0.12	0	-0.20
B	0.29	0.53	0.14	0	-0.22
	0.48	0.54	0.13	0	-0.21
	0.75	0.58	0.13	-0.01	-0.22
C	0.29	0.49	0.16	0.02	-0.25
	0.48	0.50	0.14	0.01	-0.22
	0.75	0.53	0.13	0.01	-0.22

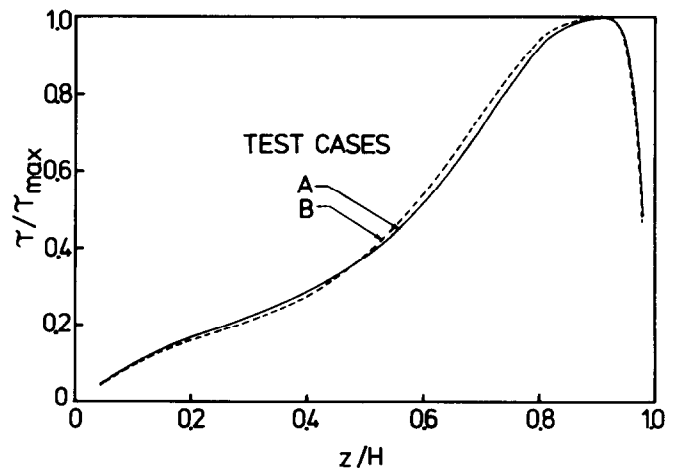


Figure 3 Predicted normalized wall shear stress for test cases A and B

Table 2 Predicted values of  $u/u$  at  $r=r_c$  for different values of  $C_1$  and  $C_2$  for test case B

C <sub>1</sub>	C <sub>2</sub>	z/H	r/R			
			0.24	0.46	0.71	0.93
1.29	1.92	0.29	0.51	0.10	-0.01	-0.17
		0.48	0.52	0.10	-0.02	-0.17
		0.75	0.57	0.13	-0.03	-0.19
1.43*	1.92*	0.29	0.53	0.14	0	-0.22
		0.48	0.54	0.13	0	-0.21
		0.75	0.58	0.13	-0.01	-0.22
1.57	1.92	0.29	0.56	0.20	0.02	-0.29
		0.48	0.56	0.16	0.01	-0.26
		0.75	0.59	0.14	0.01	-0.24
1.43	1.73	0.29	0.60	0.23	0.03	-0.34
		0.48	0.48	0.19	0.02	-0.29
		0.75	0.59	0.15	0.01	-0.26
1.43	2.11	0.29	0.49	0.08	-0.02	-0.15
		0.48	0.52	0.09	-0.02	-0.16
		0.75	0.57	0.12	-0.03	-0.19

\* Recommended by Launder and Spalding<sup>4</sup>

Computational details

The finite difference grid possessed 12 nodes in the  $z$ -direction and 15 nodes in the  $r$ -direction. The convergence was checked by ensuring that the normalized residue of all the finite difference equations be less than a preassigned

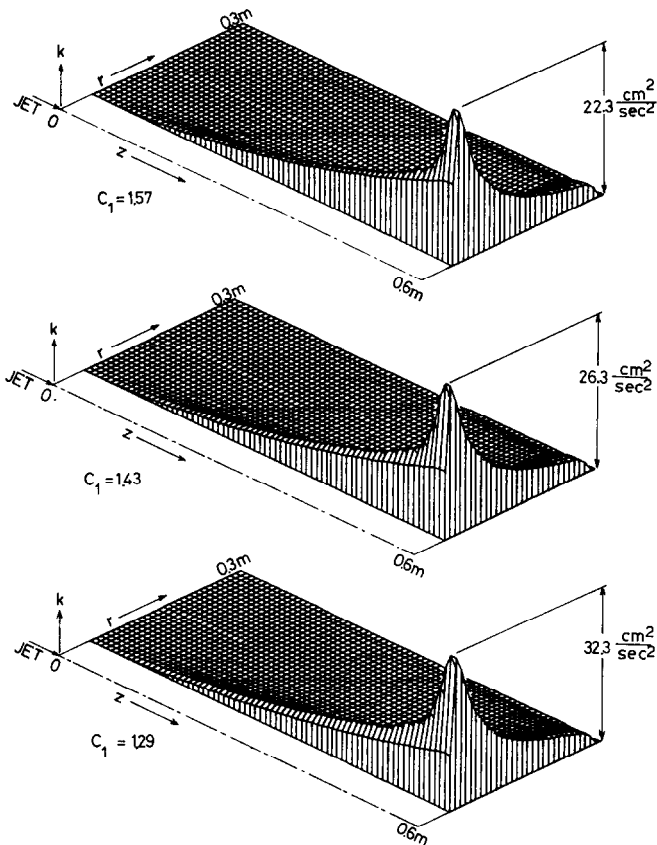


Figure 4 Effect of variation of turbulence model constant  $C_1$  on the distribution of turbulence kinetic energy  $k$  for test case B

small quantity (0.001). The computation times for test cases A, B and C are 85, 67 and 58 s respectively in a CDC 6400 computer.

### Results and Discussion

Figure 2 shows the predicted effective viscosity distribution for different boundary conditions designated by the test cases A, B and C. Regions of high effective viscosity are located in the shear layer of the jet as well as near the free surface of the liquid. These two regions are also characterized by high velocity gradients. In rest of the domain effective viscosity is relatively low which indicates a low level of turbulence.

In the absence of more detailed information on turbulence parameters in the boundary, gradient boundary condition (test case A) appears to be a reasonable specification.

Table 1 shows the effect of variation of the boundary conditions of  $k$  and  $\epsilon$  (test cases A, B and C) on the pre-

dicted  $u$  velocity field. It is observed that the effect is limited only in a limited region close to  $r = r_c$ .

Figure 3 shows the predicted wall shear distribution for test cases A and B. Predictions show region of maximum shear stress where maximum erosion can occur. It may be observed that the region of maximum shear stress is not significantly affected by the choice of the boundary conditions as given in test cases A and B.

The effect of variation of the turbulence model constants  $C_1$  and  $C_2$  on the  $u$ -velocity field is presented in Table 2. It may be noted that low velocity regions are sensitive to the turbulence model constants, however, high velocities are not significantly influenced by the imposed variation in the magnitude of the constants.

Figure 4 shows the sensitivity of a turbulence model constant on the spatial distribution of turbulence kinetic energy. High turbulence energy is located in the shear layer as well as near the free surface. The predicted maxima of turbulence energy has been found to be quite sensitive to the value of the turbulence model constants.

### References

- 1 Deb Roy, T., Majumdar, A. K. and Spalding, D. B. *Appl. Math. Modelling* 1978, 2, 146
- 2 Deb Roy, T., Majumdar, A. K. *J. Metals*, 1981, 33 (11), 42
- 3 Szekely, J., Wang, H. Y. and Kiser, K. M. *Met. Trans. B* 1976, 7B, 287
- 4 Sahai, Y. and Guthrie, R. I. L. *Met. Trans. B* 1982, 13B, 203
- 5 Launder, B. E. and Spalding, D. B. *Comput. Meth. Appl. Mech. Eng.* 1974, 3, 269
- 6 Pun, W. M. and Spalding, D. B. Heat Transfer Section Report, no. HTS/76/2, Imperial College London, 1976

### Nomenclature

$C_1, C_2, C_D$	Turbulence model constants
$G$	Turbulence energy generation
$H$	Height of water level
$k$	Turbulence energy
$p$	Pressure
$r$	Radial co-ordinate
$R$	Radius of reactor
$S_u, S_v, S_k, S_\epsilon$	Source terms for differential equation
$u$	Axial velocity component
$U$	Axial velocity at boundary
$v$	Radial velocity component
$z$	Axial co-ordinate
$\rho$	Density
$\mu_{\text{eff}}$	Effective viscosity
$\mu_l$	Laminar viscosity
$\tau$	Shear stress
$\sigma_k, \sigma_\epsilon$	Prandtl number for turbulence energy and dissipation rate